A Dual-Band and Flexible CPW-Fed Antenna for RF Energy Harvesting Applications

Alassane Sidibe, Alexandru Takacs, Daniela Dragomirescu, Samuel Charlot

A Dual-Band and Flexible CPW-Fed Antenna for RF Energy Harvesting Applications

Alassane Sidibe[1], Alexandru Takacs[1], Daniela Dragomirescu[1], Samuel Charlot[1]
[1] LAAS-CNRS, Université de Toulouse, CNRS, INSA, UPS, Toulouse, France, alassane.sidibe@laas.fr, alexandru.takacs@laas.fr, daniela.dragomirescu@laas.fr, samuel.charlot@laas.fr

***Abstract*—This paper addresses a new design of a dual-band monopole antenna on a Polyimide flexible substrate fed by coplanar waveguide technique. The final purpose of the antenna will aim to be used with a rectifier circuit as part of a rectenna for RF energy harvesting in the ISM Band. Consequently, the layout of the rectifier was considered in the simulation step. The proposed topology of this CPW-feed dual band antenna is based on a modified monopole antenna combined with a rectangular loop ring and has dimensions of 38 mm × 30 mm × 0.125 mm. Interesting performances are achieved in terms of radiation patterns. On the first band at 2.42 GHz, the maximum antenna gain is about +2.29 dBi with a quite omnidirectional pattern but in the second band, the antenna is more directive with a higher gain +3.97 dBi at 5.84 GHz.**

***Index Terms*— Flexible antenna, polyimide, dual-band antenna, rectenna, wireless power transmision, energy harvestion.**

I. INTRODUCTION

The expansion of certain electronics markets, such as medical, retail, and wearable, has significantly drawn the attention of the scientific and engineering community to the development of flexible materials, manufacturing processes and new associated electronics functionalities [1]–[3]. This is radically a game changer for the next generation of electronic devices that will no longer be limited by the integration and can match with the shape of any mount.

The benefits of using flexible electronics are multiple. Unlike the traditional rigid substrate, it is light and thin thus the weight of the electronic devices will be going to decrease considerably. It allows to reduce the size by bending or folding them according to the geometry needed. Some of these materials (such as polyactide PLA and nanocellulose-based paper) are biodegradable and other material-based polymers (PET, Polyimide, PEN…) can be easily recyclable in order to reduce the environmental footprint [4]. Furthermore, flexible electronics may require complex and costly manufacturing and assembly processes. The risk of breakage due to electronically mounted components is also high. The targeted applications for flexible electronics in this paper is Radiofrequency (RF) Energy Harvesting (RFEH) or Wireless Power Transmission (WPT). For example in the literature, a textile-based flexible rectenna is designed for wearable energy harvesting at millimeter-wave bands [5].

II. THE PROPOSED DESIGN

Basically, a rectenna stands for a *rect*ifier and an*tenna* that is used to convert electromagnetic waves to DC power in order to power supply active components such as microcontrollers, transceivers and sensors. In a rectenna, the antenna captures the EM waves (at the same frequency band) from any EM energy sources or data transmitters and provides an RF signal (P_{RF}) to the connected rectifier. An adequate matching network is used to optimize the power transfer from the output of the antenna to the input of the rectifier diode. Once the RF signal is rectified, it is then filtered to get a DC voltage that will be finally boosted, managed and stored in a storage capacitor for supplying the load. The architecture of a conventional rectenna is presented in Figure 1.

One of the main challenges of a rectenna design is the optimization of the power transmission from the antenna to the rectifier. A compact rectenna which consists of a Coplanar Waveguide (CPW) feed antenna and a microstrip rectifier connected by a 35 mm long Surface Mounted Assembly (SMA) connector and adaptor is proposed in [6]. It was clearly noted that variation between simulation and measurement results is due to soldering effects, quality of SMA connector, discontinuities of substrate dielectric constant and manufacturing tolerance. Another design of dual-band CPW rectenna first started with the design of a CPW antenna with a limited size of its ground plane and then the matching network of the CPW rectifier is modified to optimize the RF-to-DC conversion efficiency [7]. However, it is obvious that the radiation performances of such an antenna (CPW feed) will not be the same with the presence of the rectifier ground plane and would not be able to properly reach its maximum efficiency at the targeted frequency band.

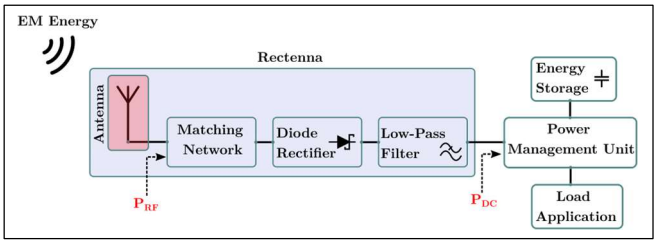

Figure 1. Schematic of a rectenna connected to a power management unit to power supply the load application with the harvested DC power from incident EM waves.

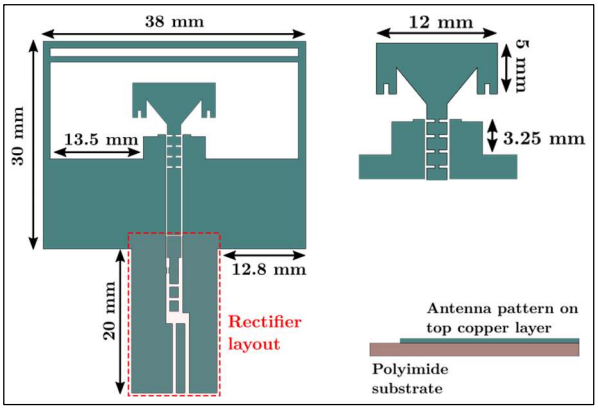

Figure 2. Layout of the proposed rectenna and side view of the design.

A 2.45 GHz broadband rectenna using a Grounded Coplanar Waveguide with a high gain of +10 dBi was presented in [8]. The drawback of this design using a 1.5 mm thick rigid substrate is the size (115 mm x 91 mm) of the use of a reflector plane at a distance of 22 mm. In our work, the final design of the proposed rectenna targeting Bluetooth and WIFI band is depicted in Figure 2. This paper will be more focused on the antenna part; its design and optimization step during simulation, and the measurement of its performances. Among all materials used for printing electronics, Polyimide material seems to be a suitable candidate as substrate thanks to its advantages (low dielectric losses, heat resistance and mechanical stability) for our needs.

III. Simulation of the Dual-Band Antenna

The antenna structure should be wisely chosen to obtain a compact design and interesting radiation performances. It can either be excited by different feeding techniques (coaxial probe, microstrip feed line, couple feed and CPW feed). The fact of using CPW feeding technique, allows the propagation of the EM field between the conduction and enable Wide-Band (WB) or dual-band features. For this purpose, an interesting CPW feed antenna at 2.45 GHz was designed with R03003 flexible material [9] and PET substrate [10]. The antenna was simulated on the Polyimide substrate (dielectric constant = 3.4; loss tangent = 0.012; thickness = 125 µm) by HFSS software from Ansys.

Two excitation/feeding approaches are used for the simulations. During the first optimization procedure of the antenna, a lumped port was used. The excitation is ensured with a Perfect Electric Conductor (PEC) bridge normal to the CPW plane and connecting the adjacent ground planes with rectangular faces (2 mm wide) as shown in Figure 3. The technique of exciting the CPW mode with air-bridge is common for antenna simulations as in [11], [12]. For highest fidelity to the manufactured sample, the RF connecter is 3D modeled and excited with a lumped port. It was previously demonstrated that this model can reliably reproduce the experimental results [13].

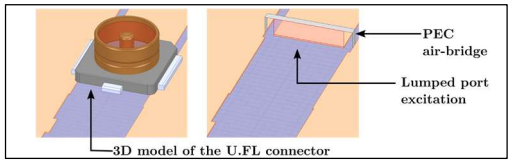

Figure 3. Feeding techniques used on the simulation.

The CPW antenna design has followed the optimization steps shown in Figure 4, Figure 5 and Figure 6. Figure 5. First, it started with a basic 11 mm length monopole antenna fed by CPW (**S1**) designed on a substrate with a size of 40 mm x 52 mm. The monopole length with a symmetrical ground plane of 11 mm x 17.75 mm presents a resonance frequency at 5.75 GHz. Then, a 70 mm length square loop element is added to connect the symmetrical ground plane in order to improve the return loss (**S2**). It can also be seen that the short-circuited loop acts as a full wavelength loop and create a resonance at 2.44 GHz as seen in Figure 4. At this step of optimization, we considered the rectifier layout. However, the transmission lines of the RF part (before the diode location) were removed to ease the use of a connector for the characterization (inset **S3**).

As expected, the rectifier layout has shifted the first resonant frequency and enhanced the bandwidth at the higher resonance mode. Therefore, improvement should be made at the first resonance created by the loop.

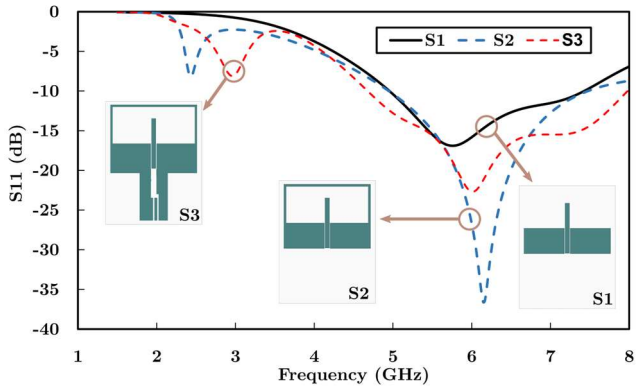

Figure 4. Simulated return loss S_{11} (dB) of the antenna at different design steps (from S1 to S3).

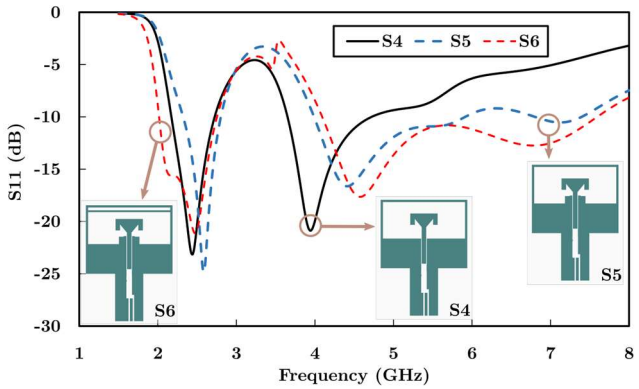

Figure 5. Simulated return loss S_{11} (dB) of the antenna at different design steps (from S4 to S6).

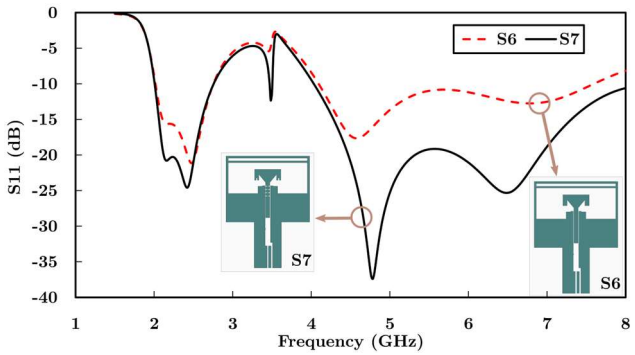

Figure 6. Simulated return loss S11(dB) of the antenna at different design steps (S4 and S6).

As seen in Figure 5, it was possible to ensure this need by changing the shape of the monopole with a triangular element on top with two rectangular arms at the ends (**S4**). On the other hand, it significantly modifies the higher resonance bandwidth that is then enhanced by adding a rectangular element on the ground plane to improve the CPW mode (**S5**). The undesired resonance around 3.5 GHz is due to the coupling between the horizontal line added for the bandwidth improvement and the head of the monopole (**S6**). Finally, short slots were added to the monopole part to improve the return loss (their length was optimized during the simulation) as seen in Figure 6.

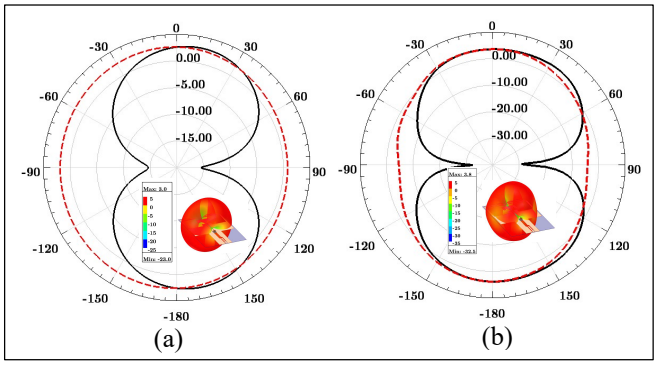

Figure 7. Simulation results of the realized gain in radiation pattern at 2.45 GHz (a) and 5.8 GHz (b) at Phi = 0 (black line) and Phi = +90° (red dashed line) ; Inset of the 3D radiation pattern (realized gain).

Figure 7 presents the simulated radiation patterns for the proposed antenna. At 2.45 GHz, the antenna radiates as an omnidirectional antenna and is more directive at high frequency.

IV. IMPLEMENTATION AND TESTS

A. *Manufactutring process of the flexible antenna*

The printing process of photolithography is the same as that used in our previous paper [13]. We use a special foil from DuPont named Pyralux AP9151R [14] to fabricate the antenna. This substrate is a 125-µm Polyimide film with a 35 µm copper foil laminated on top and bottom of it (Figure 8a).

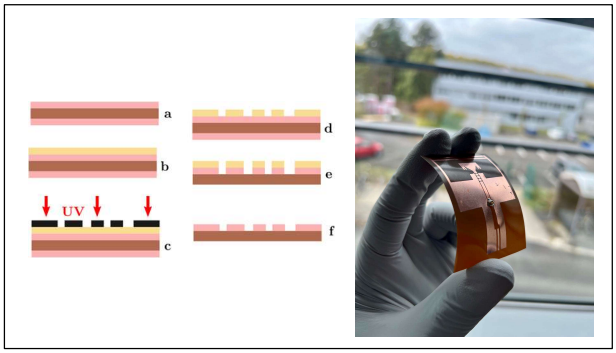

Figure 8. Description of the antenna manufacturing process (left); Photo of the manufactured antenna on polyimide substrate with a soldered U.FL connector for characterization (right).

The process flow to build the antenna is done in a clean room with photoresist equipment to allow resolution down to 10 µm. For that, a 1µm thick positive resin from Shipley (ECI 3012) is spin-coated on the substrate (Figure 8b), then bake and UV insolated through a chromium mask (Figure 8c) with the antenna design. The exposed resin then disappears in a remover (Figure 8d). The next step is the etching of the top copper not protected by the resin (Figure 8e) in a chloride iron (III) solution to minimize the lateral copper etched and keep the desired antenna layout. The back copper film is also removed at this same step. Finally, the resin is removed by acetone (Figure 8f).

The use of a U.FL connector for the characterization of such a flexible antenna is the simplest. It does not require any additional process to be assembled and can only be attached to the antenna by directly hand soldering the pads with tin.

B. *Experimental results*

The performance of the antenna is evaluated on an anechoic chamber in flat position. A U. FL to SMA adapter is connected to a cable from the Vector Network Analyzer (VNA). Figure 9 presents the comparison between the simulation done with the U.FL connector 3D model, the PEC air-bridge and the measurement. It can clearly be seen that the results fit well in the first desired region (cream color) at up to 4 GHz. The antenna is matched in a bandwidth of 690 MHz (2.06 GHz to 2.75 GHz). But there is a difference between measured and simulated return loss starting from 4 GHz. It is probably due to the inaccuracy of the measurement with the connector-adaptor at a higher frequency. The fabricated antenna stays matched under -10 dB in the band from 4.79 GHz to 7 GHz (more). The results were not plotted up to 7 GHz because of the frequency range limitation of the U.FL connector.

The gain of the antenna is measured in an anechoic chamber (by using the far-field antenna measurement facilities existing at LAAS-CNRS). A good correlation was obtained on the antenna gain as a function of the frequency with a measured gain of +2 dBi and +3.67 dBi at 2.42 GHz and 5.78 GHz, respectively (Figure 11). The radiation pattern was carried out in the E-plane where the antenna under test rotates in the azimuth plane.

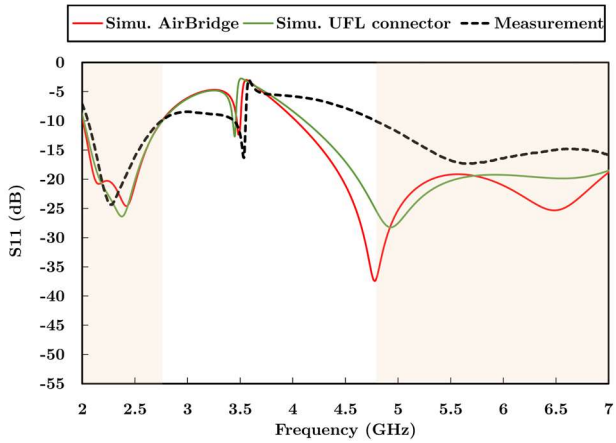

Figure 9. Comparison of the simulated return loss (with an air-bridge lumped port and U.FL) and the measurement on anechoic chamber.

As shown in Figure 11, the radiation pattern is quite omnidirectional at 2.42 GHz with a maximum gain of +2.29 dBi (Theta = +26°) and an aperture angle of 116°. The radiation pattern is a bit more directive at 5.84 GHz on some angles with a maximum gain of +3.97 dBi (Theta = -6°).

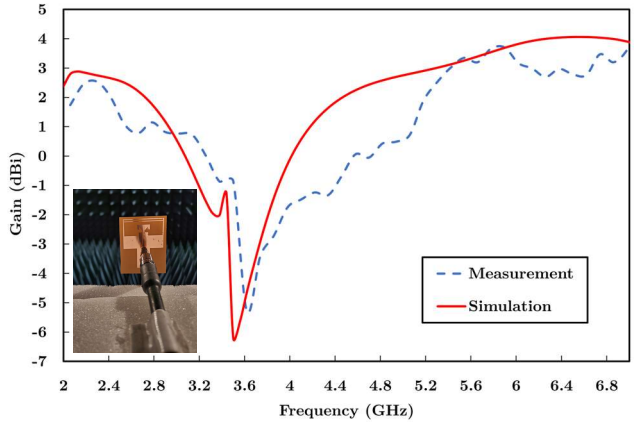

Figure 10. Comparison between measured (in anechoic chamber) and simulated realized gain (with connector) of the proposed antenna as function of the frequency on the E-plane.

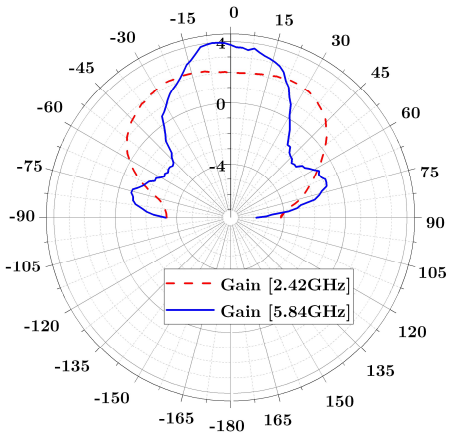

Figure 11. Measured radiation pattern in the E-plane (Phi = -90°) at 2.42 GHz (red dashed line) and 5.84 GHz (blue solid line).

V. Conclusion

In this paper, a new dual-band and flexible antenna using CPW feeding (designed for a CPW supported rectenna) has been proposed and accurately characterized. The rectifier layout has been considered during the simulation and optimizing stage. By co-designing the antenna with the rectifier layout, we can consider the electromagnetic coupling between the antenna and rectifier layout. As proved by experimental results, the proposed CPW dual band antenna covers the frequency bands (measured S11<-15 dB) of 2.08 GHz – 2.675 GHz (measured gain G> +1 dBi) and 5.29 GHz – 7 GHz (measured gain G> +2 dBi).

Acknowledgment

The authors acknowledge the French technological Network RENATECH through the LAAS-CNRS cleanroom for its support. We acknowledge UWINLOC Company and the support of the French region OCCITANIE through the research project OPTENLOC. The works were also supported by the French National Research Agency (ANR) through the McBIM Project (Communicating Material at the disposal of the Building Information Modelling), under Grant ANR-17-CE10-0014.

References

[1] C. Kallmayer, D. P. Parekh, V. Atluri, and K. Erickson, ‘New Materials and Processes for Flexible Electronics’.

[2] Z. Zhou, H. Zhang, J. Liu, and W. Huang, ‘Flexible electronics from intrinsically soft materials’, *Giant*, vol. 6, p. 100051, 2021.

[3] D. A. Corzo Diaz, G. Tostado-Blázquez, and D. Baran, ‘Flexible Electronics: Status, Challenges and Opportunities’, 2020.

[4] Z. Zhai, X. Du, H. Zheng, and Y. Long, ‘Biodegradable Polymeric Materials for Flexible and Degradable Electronics’, *Frontiers in Electronics*, p. 26.

[5] M. Wagih, G. S. Hilton, A. S. Weddell, and S. Beeby, ‘Broadband millimeter-wave textile-based flexible rectenna for wearable energy harvesting’, *IEEE Transactions on Microwave Theory and Techniques*, vol. 68, no. 11, pp. 4960–4972, 2020.

[6] Q. Awais, Y. Jin, H. T. Chattha, M. Jamil, H. Qiang, and B. A. Khawaja, ‘A compact rectenna system with high conversion efficiency for wireless energy harvesting’, *IEEE access*, vol. 6, pp. 35857–35866, 2018.

[7] M. Aboualalaa *et al.*, ‘Dual-band CPW rectenna for low input power energy harvesting applications’, *IET Circuits, Devices & Systems*, vol. 14, no. 6, pp. 892–897, 2020.

[8] M.-J. Nie, X.-X. Yang, G.-N. Tan, and B. Han, ‘A compact 2.45-GHz broadband rectenna using grounded coplanar waveguide’, *IEEE antennas and wireless propagation letters*, vol. 14, pp. 986–989, 2015.

[9] K. Aljaloud and K.-F. Tong, ‘A flexible 2.45 GHz rectenna using electrically small loop antenna’, 2018.

[10] X. Guo, Y. Hang, Z. Xie, C. Wu, L. Gao, and C. Liu, ‘Flexible and wearable 2.45 GHz CPW-fed antenna using inkjet-printing of silver nanoparticles on pet substrate’, *Microwave and optical technology letters*, vol. 59, no. 1, pp. 204–208, 2017.

[11] S.-S. Hsu, K.-C. Wei, C.-Y. Hsu, and H. Ru-Chuang, ‘A 60-GHz Millimeter-Wave CPW-Fed Yagi Antenna Fabricated by Using 0.18-μm CMOS Technology’, *IEEE Electron Device Letters*, vol. 29, no. 6, pp. 625–627, 2008.

[12] Y. Dong, T. K. Johansen, V. Zhurbenko, and P. J. Hanberg, ‘A rectangular waveguide-to-coplanar waveguide transition at D-band using wideband patch antenna’, in *2018 48th European Microwave Conference (EuMC)*, 2018, pp. 1045–1048.

[13] A. Sidibe, A. Takacs, D. Dragomirescu, S. Charlot, and J. Mennekens, 'A Novel Polyimide Flexible Antenna Design for S-Band Applications', in *2022 16th European Conference on Antennas and Propagation (EuCAP)*, 2022, pp. 1–5.

[14] DuPont Pyralux AP Flexible circuit materials datasheet [online], https://www.dupont.com/content/dam/dupont/amer/us/en/products/ei-transformation/documents/EI-10124-Pyralux-AP-Data-Sheet.pdf (accessed by 13 October 2022).